Disjoint multipath RPL for QoE/QoS provision in the Internet of multimedia things

Souhila Kettouche, Moufida Maimour, Lakhdar Derdouri

Noname manuscript No.
(will be inserted by the editor)

Disjoint Multipath RPL for QoE/QoS Provision in the Internet of Multimedia Things

Souhila Kettouche · Moufida Maimour · Lakhdar Derdouri

Received: date / Accepted: date

Abstract RPL is the IETF standardized IPv6 Routing Protocol for Low-power and lossy networks (LLNs). The major effort is therefore made on handling low data rate traffic. Meanwhile, the Internet of Multimedia Things (IoMT) emerged as one hot topic of the Internet of Things (IoT). In LLNs, providing a descent quality of service (QoS) along with a user quality of experience (QoE) for multimedia applications is challenging. High bandwidth and significant computation capabilities are necessary while LLNs are very resource constrained. To raise the available bandwidth to accommodate high data rate applications, we propose to simultaneously transmit a flow on multiple disjoint paths. To do so, we exploit the DODAG structure, already maintained by RPL, to build disjoint paths without incurring extra overhead. To reduce the amount of data to send while considering the low computation resources of video sensors, we propose to apply a priority-based low-complexity encoding scheme on the captured pictures. Highest priority data can be replicated on more than one path. Our conducted experiments using simulations as well as a real testbed show that the best QoS and QoE are obtained when multiple paths are used along with the replication of highest priority data packets.

Keywords Internet of Multimedia Things (IoMT) · RPL · Multipath routing · QoE · QoS · Cooja · IoT-Lab.

S. Kettouche
RELA(CS)^2 labs, Larbi Ben M'hidi University - Oum El Bouaghi, Algeria
E-mail: souhila.kettouche@gmail.com

M. Maimour
Lorraine University, CNRS, CRAN - 54000 Nancy, France
E-mail: Moufida.Maimour@univ-lorraine.fr

L. Derdouri
RELA(CS)^2 labs, Larbi Ben M'hidi University - Oum El Bouaghi, Algeria
E-mail: derdouril@yahoo.fr

1 Introduction

The Internet of Multimedia Things (IoMT) has experienced a tremendous development in recent years [29]. It is envisioned to play a key role in several areas such as industrial IoT, smart agriculture, smart building, smart cities and smart grid. However, IoMT applications have more stringent requirements than traditional IoT in terms of both quality of service (QoS) and quality of experience (QoE). When dealing with multimedia applications in wireless sensor networks (WSNs), one of the building blocks of the IoT, the problem becomes even more difficult. Handling high data rates is impeded by the network limited resources.

Routing Protocol for Low-power and lossy networks (LLNs), RPL is an IPv6 distance vector proactive routing protocol standardized by the IETF [3]. It builds a directed-oriented acyclic graph (DODAG) rooted at the *Sink* where each node selects a set of parents that lead to the root node based on an objective function (OF). This tree structure is motivated by the many to one delivery model that prevail in common WSNs' applications. Sensor nodes are generally in charge of reporting information to a central gateway (Sink). More interesting, this hierarchical structure reduces the size of routing tables.

Notwithstanding the fact that RPL almost meets the requirements of LLNs to support scalar data transport, it remains difficult to handle real time streaming of video clips since it was mainly targeted to low data rate applications [14]. To allow for multimedia transport, new objective functions based on energy [4, 27] or free bandwidth [8] have been proposed. These objective functions allow better performance, however, both [4] and [8] do not consider real video transmission and do not evaluate the user QoE. Authors of [27] made simulations using H. 264 multimedia trace [32] without assessing the user QoE. Besides, H. 264 compression is not suited to low-power video sensors [31].

To address the issue of bandwidth scarcity, multipath routing when carefully designed is a promising solution to aggregating the bandwidth offered by multiple paths especially in dense networks [21]. RPL multipath extension has already been considered in the literature mainly for scalar data reporting and mostly make use of braided (non-disjoint) paths [13, 17, 35]. In this paper, we propose a new extension of RPL to allow building and the use of disjoint multiple routes. Our extension uses existing RPL control messages to insure disjointness rather than leveraging the multi-instance opportunity provided by RPL as done by authors of [7]. As for [11], complete disjointness can be achieved using a detection mechanism at a common node during data transfer. This is allowed by the fact that these routes are used in a replication scenario. In our work, disjointness is guaranteed before data transmission, hence allowing for load-balancing strategies.

Extra bandwidth gained through the use of our disjoint multipath routing is not sufficient with respect to WSN's limitations. This is why, low complexity data reduction must be carried out at the video sources. This way, the quantity of the data to transmit is reduced as well as the required energy to deliver it to its final destination [15, 28]. Since widely used standard video en-

coding techniques such as MPEG-4, H.263 or H.264 do not fit sensor nodes constraints [31], we suggest to use a low-complexity video encoding technique more adapted to LLNs. We mainly make use of fast pruned DCT [24] where only a subset of its coefficients (lower frequency) are computed using optimized integer operations. In addition to this intra-frame compression, a low cost inter-frame encoding is provided to further reduce the amount of data to be reported. A priority encoding and packetization is also proposed. To compensate for the distortion caused by this so lossy compression, one may rely on the computational power of the Sink for an optimal reconstruction of the received images. Advanced reconstruction methods even based on machine learning can be applied. In our experiments, we made use of a simple algorithm [37] to inpaint the lost pixels to further improve the QoE of our multimedia application.

Our performance evaluation is conducted using both simulation and real sensor testbed (IoT-LAB [1]). We mainly assess the improvement offered by our disjoint multipath routing along with a priority-based transmission strategy when compared to one-path RPL. The traffic trace model is adopted to emulate the transmission of real video flows using an actual video encoder. Pure simulation evaluation may not fairly reproduce real-life scenarios and may not provide appropriate measures to assess the performances of a given proposal. QoS metrics such as PDR (Packets Delivery Ratio) remain pure network related measures that give limited insight into the video quality as perceived by a human and do not capture its related subjective factors. Human Perception can be assessed using QoE measures such as PSNR (Peak Signal to Noise Ratio) which can be mapped onto the MOS (Mean Opinion Score) measure and the structural similarity index (SSIM) [41].

This paper is organized as follows. An overview on the related work is given in Section 2. Then, our disjoint multipath RPL (DM-RPL) protocol is presented in Section 3. The low-complexity compression method is presented in Section 4. The evaluated scenarios and the obtained results are discussed in Section 5. Section 6 concludes the paper with some future directions.

2 Related Work

RPL [3] is the IETF standardized IPv6 Routing Protocol for Low-power and lossy networks (LLNs). Based on an objective function, each node chooses a set of parents with one designated as the preferred parent which results in a DODAG structure rooted at the *Sink*. Packets intended for the Sink are forwarded to the preferred parent. Two objective functions namely, *Minimum Rank with Hysteresis Objective Function (MRHOF)* [40] and *Objective Function Zero (OF0)* [38] are predefined. The former is based on ETX (Expected Transmission Count) metric [9] and the latter on the number of hops. The DODAG structure is maintained through the use of ICMPv6 control packets. The *DODAG Information Object* (DIO) is used to maintain the DODAG structure as it carries information that allows to select a parents set. Each

node computes its *rank*, representing its position within the DODAG, using the OF. The preferred parent for a node is the one that allows obtaining the lowest rank. The *Destination Advertisement Object* (DAO) is used to propagate destination information upward the DODAG. The *DODAG Information Solicitation* (DIS) may be used by a node to solicit a DIO or to probe its neighborhood.

Since RPL was chiefly designed to meet the requirements of LLNs, the major effort is made on handling low data rate traffic. However, modern applications are increasingly involving high speed sensing and reporting due to the growing number of sensors along with higher data acquisition frequency. Under heavy traffic, RPL may suffer from severe congestion [16]. As a result, high data loss rates, significant energy expenditure and a bad QoE are experienced especially when real time video delivery is required [14]. Based on the fact that most of losses in the presence of heavy traffic are the consequence of congestion, [16] proposed that a node chooses its parent based on queue utilization of its neighbor nodes as well as its hop count to the Sink. [34] emphasized the fact that the produced DAGs based on objective functions may not utilize the full network capacity and proposed to combine RPL object function with backpressure routing. One of the proposed algorithms is targeted to time-varying data traffic loads.

New objective functions were also proposed in the literature to allow better performance in the context of multimedia applications. The authors in [4] designed an enhanced version of RPL called Green-RPL in an attempt to minimize energy consumption. Simulation results proved that Green-RPL achieves better QoS performances in terms of energy, PDR and delay. However, the simulations are not performed using real video flows which did not allow evaluating the user QoE. In [27], a new objective function based on the remaining energy is developed. Simulation results proved that this technique extends the network lifetime compared to ETX-based RPL. However, the adopted H.264 compression technique is not suitable for sensor nodes and the user QoE was not evaluated. To meet the requirements of multimedia applications, [8] proposed FreeBW-RPL that uses a new objective function that estimates the maximum available bandwidth. Performance analyses showed that FreeBW-RPL improves upon the predefined RPL objective functions in terms of PDR, energy consumption, throughput and delay. However, once again, the authors did not consider QoE metrics that are decisive in evaluating the quality of the video received by the end users.

With regard to high data rate applications, routing protocols need to leverage the WSN density to augment its capacity by implying more nodes in the data transfer. Multipath routing is a good candidate to allow for bandwidth aggregation [6]. Load distribution in multipath routing can result in even energy consumption among sensors which improves the network lifetime by delaying the appearance of network partition. There is an abundant literature on multipath routing in adhoc wireless networks. Regarding WSNs and the particular case of a convergecast scenario, [23] leveraged the tree structure to discover extra paths with minimal overhead. As for RPL, multipath extensions have

been proposed where additional paths may serve for backup [2], balance traffic when bottleneck nodes are identified [13,19,26,43], improve reliability through replication [17] or avoid/control network congestion [20,35,42]. All the above multipath routing are opportunistic and have one hop look-ahead. More recently, to improve reliability, multipath-based replication strategies are studied in [11,17]. In [17], a *non common ancestor* alternate parent selection is proposed to allow for disjoint paths without guaranteeing complete disjointness. In [11], the *Controlled Scenario* is suggested to allow replicas that cross a common node to follow different paths which grants them disjoint paths. It is worth noting that this detection mechanism is made possible by the fact that these routes are used in a replication scenario. This cannot benefit load-balancing scenarios that aim to increase the available bandwidth rather than improving reliability. Our proposal allows to build multiple disjoint paths that can be used concurrently without requiring *common node detection* mechanism. All this without additional communication overhead.

To sum up, the above mentioned multipath RPL protocols are targeted to scalar data transfer and mostly employ braided (non-disjoint) paths. In [7], the authors exploit the multi-instance opportunity of RPL to build two disjoint paths to transport compressed video traffic. The first instance adopts MRHOF and the resulting path is used to transport the highest priority frames while the second instance uses the shortest path (OF0) to carry low priority frames. Simulation results showed that multi-instance RPL helps improving the quality of the received video based on QoS (PDR, jitter and delay) and QoE (PSNR and SSIM) metrics. However, the adopted scenario with respect to real-time streaming is unrealistic. In fact, the transmission rate is increased without raising the frames capture frequency. This does not allow a fair QoE assessment. Our real-time scenario takes into consideration the availability of the visual data to transfer. Additionally, we consider priority within each frame instead of between frames. We argue that in a real time scenario, all captured frames are of almost same importance especially when the capture frequency has already been reduced. Finally, rather than multi-instance RPL, our proposal leverages the existing RPL control messages to grant paths disjointness.

3 Disjoint Multipath RPL (DM-RPL)

High data rate applications such as multimedia ones are bandwidth demanding. Simultaneous use of multiple disjoint paths is a promising solution to offer additional bandwidth to ensure a good QoS/QoE. We propose to augment RPL without incurring much more overhead in such a way multiple disjoint paths are made available for a given source. This is why we build on the already existing DODAG structure maintained by RPL. We refer to this extension as DM-RPL for Disjoint Multipath RPL.

3.1 Network Model

We model our WSN as a connected graph $G(V, E)$ where V is the set of sensor nodes and E is the set of links connecting them. Sensors are generally in charge of reporting information to a border router (the *Sink*), $r \in V$. This delivery model is known as *convergecast* or multipoint to point communication. This is why, based on a relevant objective function, RPL builds and maintains a DODAG structure rooted at the network Sink. That is, each node x maintains its set of parents, one being designated as the preferred parent, we refer to as $\pi(x)$. When a node has to send a data packet to the Sink, it transfers it to its preferred parent. The so formed path, noted $P^+(x)$, (following child-preferred parent links) is called the *RPL path* . The obtained spanning tree of G rooted at the Sink is noted $T(V, E_T)$. Each tree rooted at a node $x \in T$ where $\pi(x) = r$ is called a *subtree* and is noted T_x. Its root x is called a *subroot*.

3.2 Paths Disjointness

The main challenge in an RPL-based multipath routing is to guarantee disjointness while keeping the related overhead as low as possible. In this paper we consider disjointness in a per source based.

Lemma 1 *In $T(V, E_T)$, a subtree T_x contains one and only one disjoint path from a source $s \in T_x$ to the root r. This path (and the corresponding subtree) can be uniquely identified by the ID of the subroot x.*

Proof (absurd reasoning) In the spanning tree $T(V, E_T)$, there is at least one path from s to r. Assume that there are two paths from s to r in the subtree T_x. The two paths will have node x as the penultimate node to reach the tree root r. This leads to non disjoint paths which is contradictory to the initial assumption.
As a subtree T_x can be uniquely identified by its root x, then the disjoint path it contains can be uniquely identified using the ID of x.■

Theorem 1 *Let u and v be two nodes in $T(V, E_T)$. If u and v belong to two different subtrees, then their respective RPL paths $P^+(u)$ and $P^+(v)$ are node disjoint : $u \in T_x \wedge v \in T_y \wedge x \neq y \Rightarrow P^+(u) \cap P^+(v) = \emptyset$*

Proof Let $u \in T_x \wedge v \in T_y \wedge x \neq y$ and assume that $P^+(u)$ and $P^+(v)$ are not node disjoint, i.e. $\exists a \in P^+(u) \cap P^+(v)$. It follows that $a \in T_x \wedge a \in T_y$ meaning that a has two preferred parents one in T_x and the other in T_y which leads to a contradiction.■

In DM-RPL, Theorem 1 is used to guarantee the disjointness of paths used by one source. Each subtree in T contains one and only one disjoint path [23]. For a given source s, to obtain disjoint paths, in addition to its RPL path $P^+(s)$, it has to designate alternate parents from disjoint subtrees. An alternate parent v (Figure 1), for instance, can be used by the source s as the

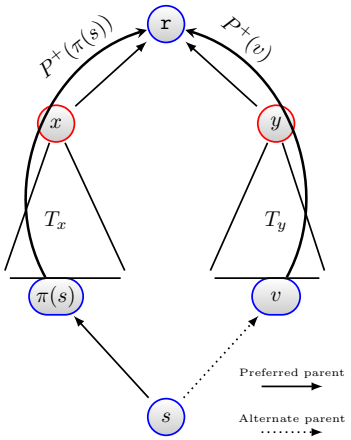

Fig. 1: Paths Disjointness

next node in another path. Node v forwards received packets via its RPL path $P^+(v)$. To be able to identify the subtree to which belong each node (based on Lemma 1), we need to propagate the ID of each subroot downward. We suggest to do that using a new field, we call PID (Path ID), in DIO messages. When a DIO from the DODAG root is received, a subroot inserts its ID in the PID field before advertising the obtained DIO to its neighbors. Upon the reception of a DIO by a regular node (other than root and subroots), it updates its parents list as suggested by default RPL but additionally it records their PID before broadcasting it as it is. When the process converges, each node will get its PID and hence will be aware of its subroot, the last node before the root as well as the parents leading to the root via disjoint paths. It is worth noting that DM-RPL correctness relies on the uniqueness of the PID. This can be achieved using any addressing (naming) scheme where simply the address of the subroot is used. The main concern is to keep the PID length as short as possible, this is why we consider an ID instead of the whole (IPv6) address. As this depends on the addressing strategy adopted in a given WSN, our choices are presented in Sections 5.2 and 5.3.

To illustrate how DM-RPL operates to propagate PIDs downward using DIO messages, thus allowing the use of multiple disjoint routes, a simple topology with a DODAG structure are shown in Figure 2(a). In this example, we note the presence of three subtrees rooted at nodes 1, 2 and 3, direct children of the root r. These nodes have chosen r as their preferred parent after receiving a DIO from it. Before broadcasting a DIO, each subroot inserts its ID in the PID field. Regular nodes (i.e. 4, 5, 6 and 7), upon the reception of such modified DIO, update the list of their parents and keep track of the corresponding PID of each parent. Node 6, for instance, has two disjoint paths via 2 and 3 respectively. Node 7 can benefit from three paths, the red one is the RPL path and the two green are the alternate paths.

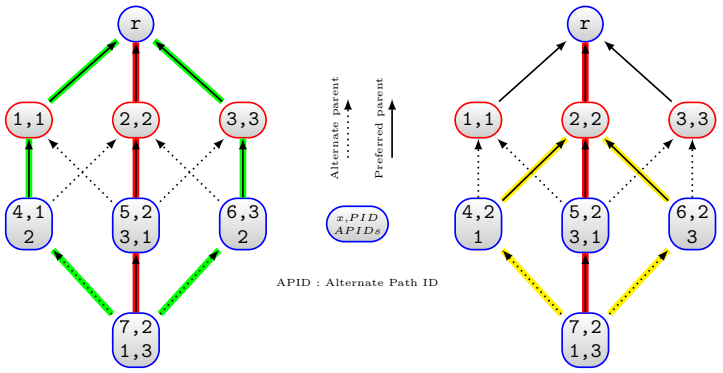

(a) 3-path scenario (b) Absence of disjoint paths

Fig. 2: Illustrative examples

3.3 DM-RPL Disjoint Paths Discovery Procedure

The above described mechanism allows to know if a path via a given alternate parent is disjoint from an RPL path. However, it does not guarantee the existence of disjoint paths for a given source. Figure 2(b) illustrates one scenario where all the parents of node 7 have the same PID. This is likely to be the case in RPL which is commonly known as the *Thundering Herd Phenomenon* [12] that occurs mainly when a node with a small rank attracts much more nodes. This motivates introducing the DM-RPL disjoint paths discovery procedure. A node x willing to send data using multiple disjoint paths that has only parents with the same PID, enters the disjoint paths discovery procedure upon the reception of Δ consecutive DIO messages. Whenever, no new PIDs are obtained during this period, the next DIO is propagated with the flag field set to $\pi(x)$, the preferred parent of this node. On the reception of a such DIO, an alternate parent (node $y \neq \pi(x)$) will replace its preferred parent by another one with a different PID than its own. For instance, in Figure 2(b), nodes 4 and 6 change their preferred parent from 2 to 1 and 3 respectively as their PID is different from their current one (i.e. 2). We thus come across the same case as in Figure 2(a).

To avoid that replacing preferred parents is made by all the neighbors which may lead to lower quality unstable paths, a parameter $\alpha \in \{0, \ldots, 10\}$ is introduced to control the trade-off between the number of disjoint paths and their quality. As the path via the preferred parent is the best one according to the adopted RPL objective function, changing to an alternate parent is not always beneficial. Hence, it is required that the change only takes place if the quality of the path via the alternate parent is above a specified threshold. Upon the reception of a DIO with the a non zero flag field, an alternate parent pull a random integer from $\{0, \ldots, 9\}$. If it is less than α, then it keeps its

preferred parent ; otherwise, it replaces it by the best alternate parent among those with a different PID than its current PID. The parameter α controls the mean ratio of the source alternate parents that have drawn to change their preferred parent. The probability that an alternate parent changes its parent is $1 - \alpha/10$. For instance, when $\alpha = 0$, all the alternate parents change their preferred parents to obtain a different PID. In a dense network where a node is likely to have a large number of neighbors, it is more interesting to increase the value of α as to bound the number of alternate parents that change their preferred parent. Increasing the number of paths through preferred parents substitution would lead to lower quality (possibly longer) paths which may result in a decrease of the multipath overall performance. Let reconsider Figure 2(b). Assume that α is set to 5 and that nodes 4 and 6 pull 2 and 7 respectively, then node 4 will keep its PID while node 6 will change its preferred parent from 2 to 3. In this case, we obtain two disjoint paths instead of three. Further analysis of DM-RPL behavior with respect to α and Δ parameters is done by simulation in Section 5.1. Algorithm 1 summarizes the main actions of DM-RPL.

3.4 Discussion

To handle multimedia applications, one has to deal with the issue of bandwidth scarcity in WSNs. Therefore, we considered the use of multiple disjoint paths to obtain additional bandwidth. Also, multipath routing distributes the communication load on a larger number of nodes. This results in a more even energy consumption which may increase the network lifetime. Lastly, multipath allows multimedia traffic to be prioritized on a per-path based strategy. Compared to non-disjoint (opportunistic) multipath, disjointness requires more information to be satisfied. The probability of finding disjoint paths is lower, which requires a minimal network density. In sparse networks, finding disjoint paths is more difficult. When multiple routes are not available, the source simply uses the RPL path and thus operates in degraded mode.

The main idea in this work is to take advantage of a tree structure to build disjoint paths to meet the bandwidth needs of a multimedia application. The tree structure allows for small-state routing. Instead of implementing from scratch all the operations required to build and maintain the tree structure, we chose to use the DODAG structure provided by RPL. Any other tree-base protocol could have been used. RPL is chosen since it is considered as the *de facto* IoT routing protocol. Improving RPL is a hot research topic, more and more efforts are made to allow for IoMT using RPL (Section 2).

3.4.1 DM-RPL Cost

As DM-RPL builds on an already existing routing protocol, we consider here the additional cost incurred by our multipath protocol with respect to RPL in terms of both communication and processing overhead. In DM-RPL, there is

Algorithm 1: DM-RPL

Data:
x is this node and $\Pi(x)$ is its parents set;
$\pi(x) \in \Pi(x)$ is the x's preferred parent. Let $\Pi^*(x) = \Pi(x) - \pi(x)$;
$\Delta \geq 2$, the minimum number of DIO a source receives before entering the DM-RPL disjoint paths discovery procedure;
$\alpha \in 0..10$, a trade-off parameter that mainly controls the replacement of the preferred parent;
Each regular node maintains an additional field PID for each parent entry in the neighbors table. This is referred to as $y.PID$ for $y \in \Pi(x)$;

Result: Two disjoint paths for a given source. The generalization to more paths is straightforward

The root broadcasts the initial DIO message with $DIO.PID \leftarrow 0$ and $DIO.flag \leftarrow 0$;

Upon the reception of a DIO :
handle the DIO as in default RPL
if $\pi(x) = r$ **then** `// I am a subroot`
  broadcast the DIO with $DIO.PID \leftarrow x$

if $\pi(x) \neq r$ **then** `// I am a regular node`
  if $DIO.flag = 0$ **then**
    broadcast the DIO as it is : $DIO.PID$ field set to this node subroot
  else `// Enter the DM-RPL disjoint paths discovery procedure`
    pull a random integer number $rdm \in 0..9$;
    if $rdm \geq \alpha$ **then**
      let y^* be the best parent of x in $\Pi^*(x)$ with $y.PID \neq x.PID$, then $\pi(x) \leftarrow y^*$;
      broadcast the next DIO with $DIO.PID \leftarrow y^*.PID$

A source (regular) node willing to transmit data using multipath :
The first path is the one that follows the preferred parent i.e. via $\pi(x)$;
$countDIO \leftarrow 1$;
if $\exists y \in \Pi^*(x)$ *with* $y.PID \neq x.PID$ **then**
  choose the best parent y^* to be the next hop for the second disjoint path
else
  wait for a new DIO;
  $countDIO \leftarrow countDIO + 1$;
  if $countDIO < \Delta$ **then**
    if $\exists y \in \Pi^*(x)$ *with* $y.PID \neq x.PID$ **then**
      choose the best y^* to be the next hop for the second disjoint path
  else `// Trigger DM-RPL disjoint paths discovery procedure`
    broadcast the next DIO with $DIO.flag \leftarrow \pi(x)$

no additional messages since we make use of the already existing DIO messages. Moreover, no extra fields are added, the flag and two unused 1-byte fields in the DIO message are used to store the $flag$ and the PID required for the effective operation of DM-RPL. Additional processing is limited to the "DM-RPL disjoint paths discovery procedure" triggered every "Δ" DIO messages whenever the current configuration does not allow for the required number of paths. The source has to maintain and update a counter. The procedure is then executed by the source's alternate parents with a probability $1 - \alpha/10$. This gives an idea on the frequency of performing such a procedure that remains of a limited complexity since it consists in invoking a function that chooses the second best parent in the parents list. Simulation based results presented in Section 5.1 give other elements to get more insight on the frequency of this procedure.

3.4.2 Routes Maintenance

As DM-RPL builds on RPL, the former relies on the latter maintenance and repairing strategies. This motivated extending RPL instead of implementing a new tree-based multipath routing protocol. To maintain the DODAG structure, repair mechanisms are provided by RPL. For instance, when a node detects a network inconsistency, it can trigger a local repair that consists in urgently finding a backup path without trying to repair the whole DODAG. In some circumstances, a global repair can be initiated by the DODAG root. Note that due to network dynamics, transient periods where paths disjointness cannot be guaranteed may occur. Hence, built paths are subject to changes since they have to follow the DODAG structure. With respect to disjoint multipath maintenance, it is the responsibility of the source to ensure that the used parents always belong to different subtrees.

3.4.3 Multiple Sources

The main focus of DM-RPL is to propose multiple disjoint paths for one source in a DODAG structure. The protocol can be generalized to multiple sources using some additional mechanisms that have to be effective while being of low cost. One solution consists in isolating each already used subtree as proposed in [23]. This being said, one can relax inter-session disjointness as to reduce the associated overhead. Instead, one can rely on an appropriate objective function that avoids overloaded nodes. The OF we chose in our performance evaluation is based on ETX that tends to avoid overloaded nodes and less quality links.

4 Priority-based Low Complexity Visual Data Reduction

Authors of [5] have shown that using multiple routes allows doubling the overall throughput. Nevertheless, a descent video quality was difficult to obtain

even when capturing and transmitting at only 6 fps a gray-scale low resolution video compressed using MPEG-4. This is due to the limited capacity of an LLN network. Even with multiple paths, it is still difficult to provide enough bandwidth to meet the needs of data intensive applications that are often encountered in the IoMT. Having sensors to deliver all the visual data captured is inefficient and should be avoided. Therefore, in-network data reduction is definitely needed to reduce transmissions. As mentioned earlier, MPEG-4 is not adapted to low power video sensors. Not even the low complexity JPEG still image compression algorithm. This is mostly driven by the discrete cosine transform (DCT) step [33,36]. In order to accommodate the limited computational capabilities of low-power video sensors, we suggest using a priority-based low complexity image compression method [22].

A captured frame is encoded as a main (M) or a secondary frame (S). An M-frame is intra-coded and an S-frame is inter-coded where only the difference with the previous M-frame is encoded. The choice between M and S encoding depends on a parameter, g, we call the GOP coefficient. If the mean square error (MSE) with respect to the previous M-frame is less than g^2, then the frame is S-encoded ; otherwise, it is M-encoded. Note that if $g = 0$ then we get all M-frames. Raising its value produces more S-frames which reduces the data transmission rate. A lossless entropy encoding is applied at the last step for both M- and S-frames.

4.1 Main Frame Encoding

Figure 3a shows the steps of encoding an M-frame. The image is first decomposed into 8×8 blocks. Then, a fast pruned DCT called binDCT-C [18] is applied on each block with a triangular pattern [25]. Only coefficients located at the upper left triangle of side length $\rho \leq 8$ are considered. This is done to reduce the DCT computational complexity as well as the amount of data to encode and transmit. The resulting DCT block coefficients are quantized using the JPEG standard quantization matrix. A quality factor (QF) that allows adjusting the quantization matrix values can be adjusted to control the trade-off between the compression rate and the obtained quality. The resulting block is then linearized following a zigzag scan and a priority mechanism is implemented. Since the useful signal information is concentrated in the lower DCT coefficients, we propose to divide each block coefficients into two levels. The highest priority level is composed of the DC component (b_{11}) and the following two AC components (b_{12} and b_{21}). The remaining coefficients of the block are put in the low priority level.

4.2 Secondary Frame Encoding

As shown in Figure 3b, the difference between the current frame and the previous M-frame is divided into 8×8 blocks. Then, a MOS-based prioritization

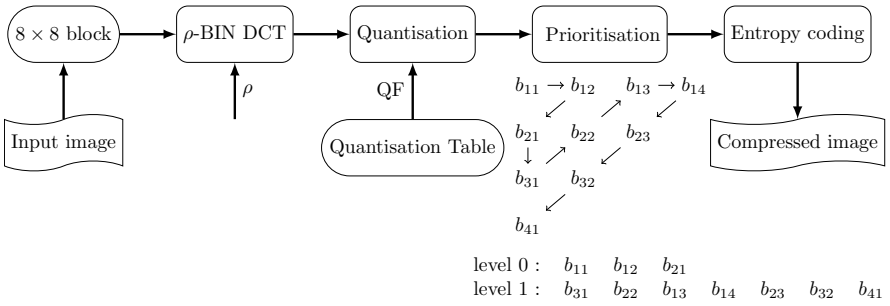

(a) M-frame

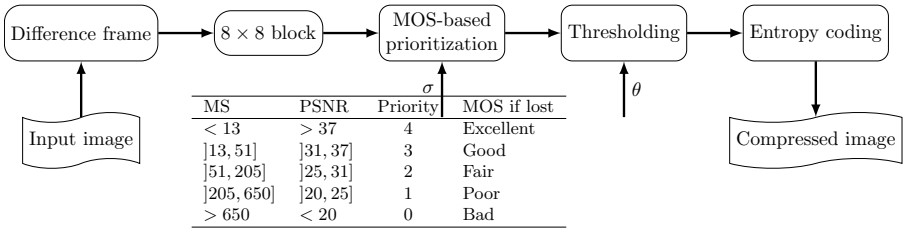

MS	PSNR	Priority	MOS if lost
< 13	> 37	4	Excellent
$]13, 51]$	$]31, 37]$	3	Good
$]51, 205]$	$]25, 31]$	2	Fair
$]205, 650]$	$]20, 25]$	1	Poor
> 650	< 20	0	Bad

(b) S-frame

Fig. 3: Low-complexity Compression Scheme

scheme is performed on each difference block d. Based on its mean square $MS = \sum d_{ij}^2/64$, a mapping is established to characterize the quality we would obtain if this block is lost. For instance, the highest priority is given to blocks with $MS > 650$. If such a block is lost, then when reconstructed based on the previous M-encoded block, it will obtain a bad quality with a $PSNR < 20$ dB. To further save video sensors and network resources, a thresholding is applied on the obtained blocks where values less than θ, a *threshold similarity* parameter, are simply zeroed.

4.3 Frames Reconstruction at the Sink

Data reduction combined to multipath transmission do not avoid data packet losses due to the constrained nature of our target network. When the Sink reconstructs the images based on the received packets, bands of damaged pixels appear. In order to fill in the lost pixels in an image, we propose to benefit from a digital inpainting algorithm. We adopted the simple and fast algorithm of Telea [37] based on the fast marching method for level set applications.

5 Performance Evaluation

To conduct our performance evaluation using both simulation and real experimentation, we extended the Contiki 3.0 implementation of RPL [10]. Real video clip transmission is emulated through the use of traffic trace file (*st-packet*) generated by SenseVid [22], a tool for QoE video transmission evaluation in WSN. The RPL-UDP sender application is modified to enable the transmission of packets according to the instructions (from the traffic trace file) received via the serial connection. Similarly, the receiver modules is modified to enable the retrieve, via the serial connection, the list of received packets to store in a receiver trace file (*rt-packet*). SenseVid, based on the list of received packets, reconstructs the images considering the experienced losses. QoE video related measures are computed. The PSNR between the original captured image and the received, possibly distorted frame is given by :

$$PSNR = 20\ log\ \frac{V_{peak}}{MSE}$$

where V_{peak} is the maximum possible pixel value. The SSIM metric based on the degradation of structural information allows measuring the similarity between the captured frame and the received one. It assumes that the human visual perception is highly adapted for extracting structural information from a scene [41] :

$$SSIM = \frac{2\mu_x\mu_y + C_1}{\mu_x^2 + \mu_y^2 + C_1} \times \frac{2\sigma_x\sigma_y + C_2}{\sigma_x^2 + \sigma_y^2 + C_2} \times \frac{\sigma_{xy} + C_2/2}{\sigma_x\sigma_y + C_2/2}$$

where x and y are non negative image signals, μ_x, σ_x and μ_y, σ_y are the mean and standard deviation of x and y respectively. σ_{xy} is the sample cross-covariance between x and y. $C_1 = 6.5025$ and $C_2 = 58.5225$. In addition to the QoE metrics, we consider in our performance evaluation, traditional QoS metrics such as energy and PDR (packet delivery ratio). Each experiment is repeated at least 20 times to avoid fluctuation.

To get insight into the performances of our disjoint multipath extension, we made extensive simulations using Cooja [30], the Contiki network simulator. We began by studying some properties of our multipath discovery procedure with respect to its parameters α and Δ. Then, the performances of DM-RPL are assessed with respect to standard RPL. Finally, real time video frames transmission is considered in real testbed experiments.

5.1 Preliminary Analysis

In order to get some insights into the behavior of DM-RPL with respect to the required time to obtain additional paths and their number, we performed simulations using a random topology of 25 sensor nodes distributed in a square area of side $120m$. The propagation model is a Unit Disk Graph Model with a

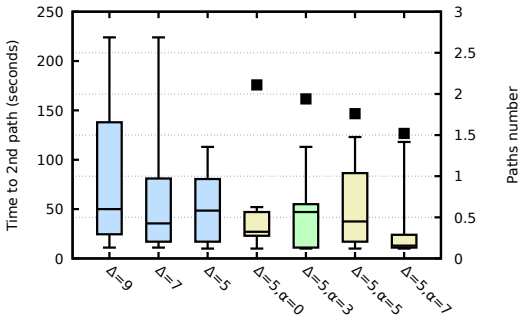

Fig. 4: DM-RPL parameters (α and Δ) impact

transmission range of $45m$ which results in a mean degree (number of neighbors) of 3.2 for each node. Despite the fact that our multipath protocol allows to build more paths, with such a density, we used only two paths to be able to perform a sufficient number of experiments. The source node obtained at least 2 paths in more than 50% of the simulations for $\Delta = 5$. When the DM-RPL disjoint path discovery procedure is triggered, the source is able to get at least 2 paths in all the simulations when $\alpha = 0$. When α is increased to 3, 5 and 7, the source gets at least 2 paths in 88%, 76% and 53% of cases respectively.

Figure 4 shows using box plots the required time to get the second path when the DM-RPL disjoint discovery procedure is triggered for different values of Δ and α. The number of built paths is depicted using black squares when α is varied. As expected, the number of paths decreases when α is increased. Moreover, the required time to get a second path increases with Δ. Although in half of the cases, this delay remains below 50 sec, it can rise to high values. Note that this delay bounds (minimum and maximum values) depend on the min/max DIO intervals set to their default values (4 sec and 17.5 min, respectively) in our simulations. When these latter are set to lower values, we can consider rising Δ. In order to reduce the convergence time, one can consider the use of the DIS-Trickle mechanism in a selective (both temporal and spatial) way to accelerate the convergence of the multipath routing.

5.2 Simulation Results

In this section, Cooja simulations are performed with the aim of comparing DM-RPL using two paths with default RPL. In cooja, the least significant bytes of the IPv6 address are set to the ID of a node that corresponds to the order in which the node was created. To designate a disjoint path, we use as a PID, the ID of the corresponding subroot. The sent traffic corresponds to 25 gray-scale images (giving a frame capture rate of 2 fps) extracted from the 300 frames that composes the *hall monitor* video clip [39]. To further fit the LLN limited capacity, we consider down-sampling the images to 128×128

Table 1: Simulation Parameters

Operating system	Contiki OS	Packet max. payload	128 Bytes
Sensors type	Tmote Sky	Transport protocol	UDP
Number of sensors	25	Routing protocol	RPL, DM-RPL (IPv6)
Area	120 $m \times 120$ m	DIO min/max intervals	4 sec/17.5 min
Transmission range	45m	RPL objective function	MRHOF
Interference range	50m	DM-RPL default param.	$\Delta = 5$, $\alpha = 3$
MAC	CSMA	Radio Duty Cycling	ContikiMAC
		Channel check rate	128 Hz
Video duration	12 seconds	Quality Factor	20
Frame resolution	128x128	DCT	Triangular ($\rho = 8$) BIN DCT
Frames per second	2	Number of priority levels	1, 2
Number of frames	25	Entropy coder	Exponential-Golomb (EG)

resolution. In these simulations, all the captured images are encoded independently of each other (M-encoded). We consider two main scenarios. First, all the packets get the same priority and are sent without differentiation. In the second scenario, two levels of priority are used and packets with higher priority are sent twice by the source, each on one path in the case of DM-RPL. A contention-based CSMA MAC protocol is used to avoid collisions. At a higher layer, the OF when appropriately chosen can also play a role in avoiding packet losses. We considered the MRHOF in this work. Table 1 summarizes the simulation parameters.

Figures 5a-5b show respectively the distribution and mean PDR obtained by RPL (1-path) and DM-RPL (2-path) for one ($l1$) and two ($l2$) priority levels when the transmission rate is varied from 1 to 5 packets per second (pps). While the mean PDR decreases for all scenarios, we note that with two priority levels, we obtain better performances in both RPL and DM-RPL. This is due to the replication of a subset of the data packets which results in an improved reliability. Besides, using two paths allows obtaining higher PDR with or without replication. DM-RPL allows getting more bandwidth thanks to data splitting on two disjoint paths. We observe that the priority-based scenario coupled with multipath routing obtains the highest PDR with values more concentrated around the median.

Figures 5c-5f depict the quality of the received images as reconstructed by SenseVid considering the experienced packet losses. When the transmission rate is low as 1 pps which results in a very low loss rate, we note that the obtained quality is close to that of the transmitted (reference) frames mainly for DM-RPL. Note that the reference PSNR and SSIM are respectively 34.0920 dB and 0.9629. When the transmission rate is increased the quality deteriorates due to the experienced losses. We observe, however that the quality is improved when higher priority packets are replicated ($l2$) regardless of the number of used paths. This is more noticeable when two paths are used. In fact, we observe that the minimum quality obtained using DM-RPL with two priorities is always higher than the maximum quality obtained by

one path and one priority. Paths diversity reduces losses and important visual data success transmission is likely to be maximized with replication of higher priority packets.

Figure 6 shows visual samples of frame 22 with the corresponding PSNR and SSIM when transmitted at 4 pps. The rightmost one is the reference frame transmitted by the source. The other images are those received by the Sink when using the different transmission scenarios. We observe that the image that corresponds to the first scenario (1 path and 1 priority level) is useless. When using 2 paths along with replication of higher priority packets, we are able to distinguish the man walking in the corridor.

Finally, to get some insight on the impact of our transmission strategies on energy, we represent the distribution and mean values of the consumed power by the radio for transmission. Figures 5g-5h show that transmitting at a higher rate consumes more energy especially when only one path is used. More interesting, we observe, for higher data rates, a significant increase in power consumption when replication is used with RPL while it remains mostly the same with DM-RPL. Our multipath protocol allows obtaining the lowest energy expenditure especially for high data rates. This is mainly due to the absence of retransmissions due to an improved reliability as shown by PDR curves.

5.3 Experimental Results

In this section, we compare DM-RPL to default RPL by focusing on the impact of increasing images frequency capture on their real time transmission. To do so and coping with the limitations of the used sensors, we consider the transmission of only 9 to 18 gray-scale images of the hall monitor video. Moreover, we lower the quality factor to 5. To further reduce the data transmission rate as shown in Table 2, we include some S-frames by setting the GOP coefficient g to 15. σ is set to zero so only their highest priority level data are encoded and transmitted. The threshold similarity θ is set to 1. All the resulting packets are assigned the same priority level.

Our real experiments are made using IoT-LAB [1], an open experimental IoT testbed composed of thousands of nodes distributed over six sites in France. We made use of 15 M3 open nodes[1] located at the F4 corridor of Grenoble site. In order to be able to find disjoint paths in DM-RPL, we need to propagate downward the PID that must uniquely designate each subroot in the DODAG. We used in our implementation, the last two bytes of the IPv6 address of each subroot. The PID uniqueness is guaranteed since only these bytes are varied in the IPv6 address assignment and sub-netting in IoT-LAB testbeds. The unused 7^{th} (*Flags*) and 8^{th} (*Reserved*) bytes of the DIO packet are chosen to constitute the PID field. We access the IoT-LAB testbed using provided command-line tools and retrieve our experiments results using serial

[1] https://www.iot-lab.info/docs/boards/iot-lab-m3/

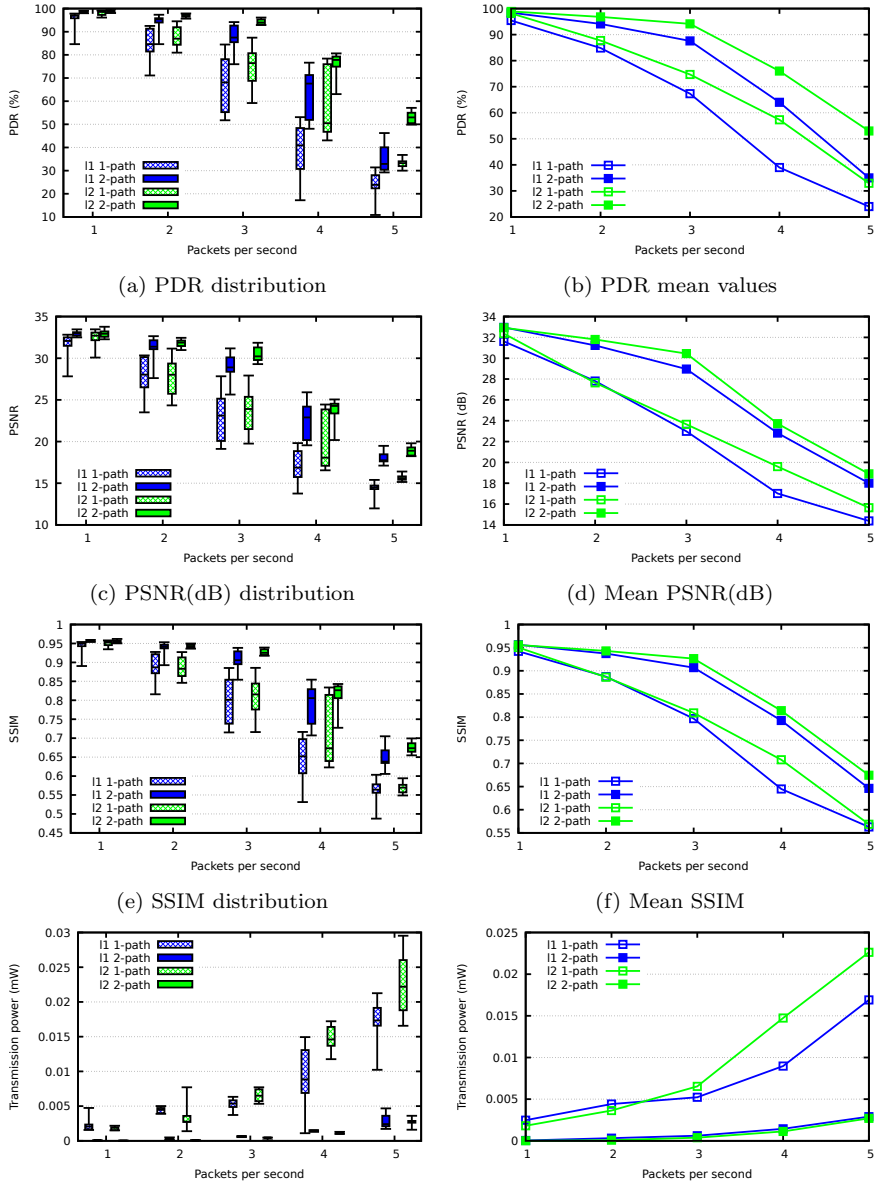

(a) PDR distribution

(b) PDR mean values

(c) PSNR(dB) distribution

(d) Mean PSNR(dB)

(e) SSIM distribution

(f) Mean SSIM

(g) Transmission Power (mW) distribution

(h) Mean Transmission Power (mW)

Fig. 5: Simulation results

(a) Reference	(b) l1 1-path	(c) l1 2-path	(d) l2 1-path	(e) l2 2-path
PSNR 34.244	17.315	22.416	20.841	24.030
SSIM 0.9620	0.6650	0.7940	0.7610	0.8400

Fig. 6: Sample images for frame 22 when transmitted at 4 packets per second.

Table 2: Transmitted video characteristics (IoT-LAB)

Images	ref. PSNR (dB)		ref. SSIM		compression (bpp)		bit rate (Kbps)		packets to send		Frames sequence
number	$g=0$	$g=15$	$g=0$	$g=15$	$g=0$	$g=15$	$g=0$	$g=15$	$g=0$	$g=15$	when $g=15$
9	29.50	28.52	0.9081	0.8980	0.66	0.57	7.8	6.73	99	90	MMMMSMSMS
12	29.50	28.81	0.9010	0.8997	0.66	0.57	10.40	8.98	132	116	MMMMMSMMSMSM
15	29.50	28.05	0.9077	0.8959	0.66	0.52	13.01	10.32	165	140	MSMMMMSMSMSMSSM
18	29.51	28.31	0.9078	0.8960	0.66	0.51	15.6	11.94	198	162	MSMMMSMSSMSMSMSSMM

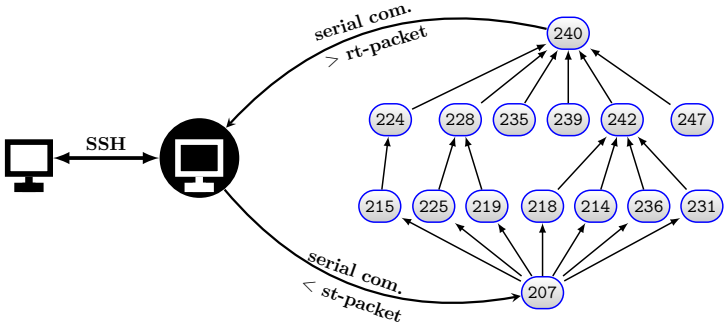

Fig. 7: IoT-lab Experiment Setup and Interface with SenseVid.

ports. Figure 7 shows how transmission instructions based on st-packet file are given to the source (node 207) that sends in a real time the captured images to the root (node 240). A possible tree structure is also shown where the links are those connecting each node to its preferred parent.

Figure 8a shows the mean PDR obtained when RPL and DM-RPL are used to send the two sequences of frames ($g0$ and $g15$). We observe that the PDR decreases when the number of images to transmit is increased. This was expected since the data rate transmission is increased. DM-RPL outperforms RPL in terms of PDR whatever the transmission rate. Reducing the transmission rate by inter-coding some frames ($g = 15$) allows achieving higher PDR with respect to the case where all frames are intra-coded ($g = 0$). This observation applies for both RPL and DM-RPL.

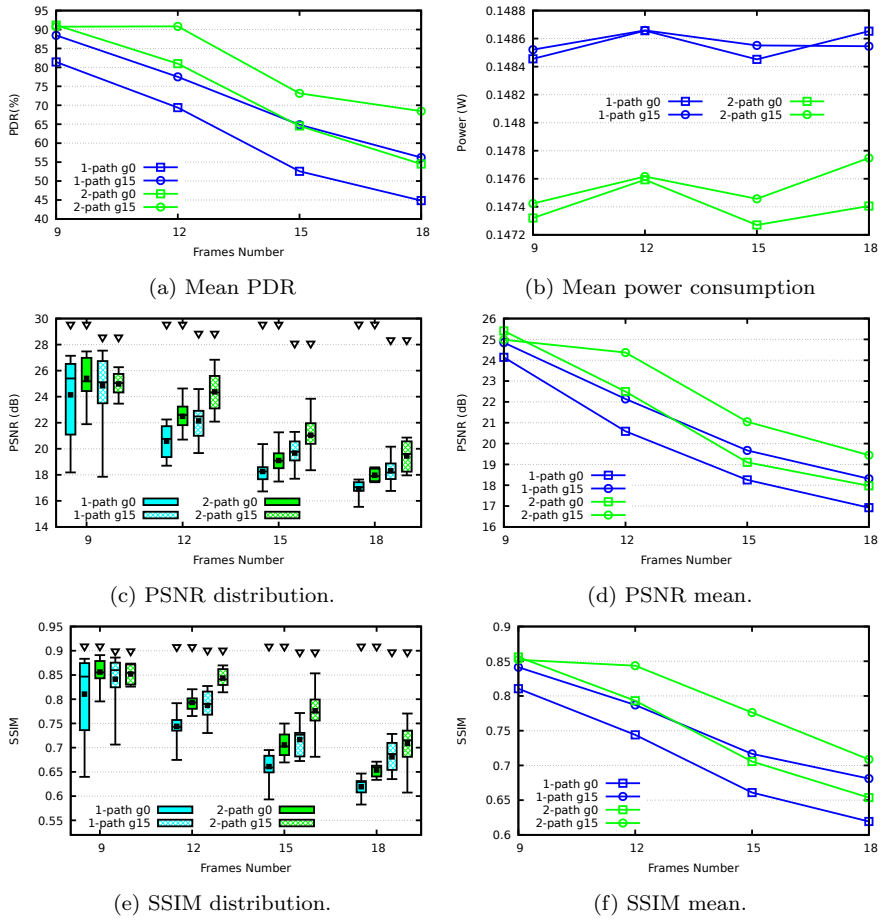

(a) Mean PDR

(b) Mean power consumption

(c) PSNR distribution.

(d) PSNR mean.

(e) SSIM distribution.

(f) SSIM mean.

Fig. 8: IoT-LAB experimental results

Figure 8b depicts the mean consumed power for the different schemes as a function of the number of captured frames. Compared to RPL, DM-RPL consumes lower amount of energy. This is the consequence of traffic load balancing when using DM-RPL. Lower packet losses are experienced and thus reducing the amount of MAC level retransmissions. This translates in lower energy consumption.

Figures 8c-8f show mean and distribution plots of the obtained PSNR and SSIM of the received images by the Sink. Triangles in the box plot depict the reference PSNR and SSIM. Data reduction due to the introduction of S-frames brings lower image quality with respect to the use of only M-frames as shown by the reference PSNR and SSIM in Table 2. We note that the quality is lowered when increasing the transmission rate. The images quality is still fair ($PSNR > 20$) for all schemes when the number of frames does not

(a) Reference	(b) 1-path, g0	(c) 2-path, g0	(d) 1-path, g15	(e) 2-path, g15
PSNR 29.530	20.180	22.185	19.819	24.319
SSIM 0.907	0.747	0.802	0.767	0.850

Fig. 9: Sample images for frame 3 when 12 frames are captured.

exceed 12. Using two paths with more data reduction (2-path, $g15$) allows an acceptable quality even for the highest transmission rate. Note that thanks to data reduction, received images quality is better when $g = 15$ compared to $g = 0$ even if the corresponding reference values are higher in the latter case. Figure 9 shows the third transmitted frame when 12 images are captured and transmitted with samples of the same frame as received by the Sink for the different evaluated schemes. Observing the pictures confirms that data reduction strategy is profitable mainly when two paths are used where both PSNR and SSIM are improved.

6 Conclusion

In this paper, a disjoint multipath extension of RPL called DM-RPL is proposed as well as a low complexity data reduction at the video source as an attempt to support multimedia traffic in low-power and lossy networks. Paths disjointness is guaranteed at the source before starting transmission without incurring additional overhead. Moreover, an intra-frame priority mechanism is implemented at the encoding and packetization steps. At the Sink side, an inpainting algorithm is used to allow recovering lost pixels.

We carried out experiments using both simulation and real WSN testbed along with real video clip transmission. We considered both QoS (packet delivery ratio and energy) and QoE (PSNR and SSIM) to assess the performance of our proposal mainly compared to standard RPL. We proposed to replicate high priority packets which are sent on two paths. Our results show that using two paths along with the priority mechanism achieves the highest performances. On the one hand, multiple paths allow to gain more bandwidth when compared to one path. On the other hand, highest priority packets delivery ratio is improved which results in reconstructed images with better quality. Energy expenditure is also reduced.

Despite the obtained results, there is still room for improvement regarding the QoE from the received images. As a future work, we expect to improve the rate-distortion efficiency of our compression strategy while remaining low-complex. Transmission strategies involving interleaving techniques along with

advanced deep learning methods for image reconstruction with denoising and supperresolution are under study. Regarding the multipath routing algorithm, we expect to leverage the *DIS-Trickle* mechanism to accelerate the discovery process of additional paths. The case of inter-session paths disjointness needs to be addressed. A more in-depth theoretical analysis of DM-RPL is to be carried out. This is mainly to get more formal proofs of our protocol correctness and complexity as well as studying the impact of its different parameters. Moreover, we plan to conduct more extensive simulations to assess the scalability of DM-RPL to large networks and the impact of network density and dynamics on its performance as well as the impact of adding more paths as to deduce their optimal number with possible presence of multiple sources.

Acknowledgement. Authors thank FIT IoT-LAB project for providing testbed and tools to perform this paper experiments.
This work was supported in part by the PHC TASSILI 21MDU323.

References

1. Adjih, C., Baccelli, E., Fleury, E., Harter, G., Mitton, N., Noel, T., Pissard-Gibollet, R., Saint-Marcel, F., Schreiner, G., Vandaele, J., et al.: Fit iot-lab: A large scale open experimental iot testbed. In: 2015 IEEE 2nd World Forum on Internet of Things (WF-IoT), pp. 459–464. IEEE (2015)
2. Ahrar, E.M., Nassiri, M., Theoleyre, F.: Multipath aware scheduling for high reliability and fault tolerance in low power industrial networks. Journal of Network and Computer Applications **142**, 25–36 (2019)
3. Alexander, R., Brandt, A., Vasseur, J., Hui, J., Pister, K., Thubert, P., Levis, P., Struik, R., Kelsey, R., Winter, T.: RPL: IPv6 Routing Protocol for Low-Power and Lossy Networks. RFC 6550 (2012). DOI 10.17487/RFC6550. URL https://rfc-editor.org/rfc/rfc6550.txt
4. Alvi, S.A., Shah, G.A., Mahmood, W.: Energy efficient green routing protocol for internet of multimedia things. In: 2015 IEEE Tenth International Conference on Intelligent Sensors, Sensor Networks and Information Processing (ISSNIP), pp. 1–6. IEEE (2015)
5. Bidai, Z., Maimour, M.: Interference-aware multipath routing protocol for video transmission over zigbee wireless sensor networks. In: IEEE (ed.) the 4th International Conference on Multimedia Computing and Systems. IEEE, Marrakesh, Morocco (2014)
6. Bidai, Z., Maimour, M.: Multipath routing for high-data rate applications in zigbee wireless sensor networks. In: the 6th International Conference On New Technologies, Mobility & Security (NTMS'2014), pp. 1–5 (2014)
7. Bouacheria, I., Bidai, Z., Kechar, B., Sailhan, F.: Leveraging Multi-Instance RPL Routing Protocol to Enhance the Video Traffic Delivery in IoMT. Wireless Personal Communications pp. 1–30 (2020)
8. Bouzebiba, H., Lehsaini, M.: FreeBW-RPL: A New RPL Protocol Objective Function for Internet of Multimedia Things. Wireless Personal Communications pp. 1–21 (2020)
9. De Couto, D.S.J., Aguayo, D., Bicket, J., Morris, R.: A high-throughput path metric for multi-hop wireless routing. In: Proceedings of the 9th ACM International Conference on Mobile Computing and Networking (MobiCom '03). San Diego, California (2003)
10. Dunkels, A., Gronvall, B., Voigt, T.: Contiki - a lightweight and flexible operating system for tiny networked sensors. In: 29th annual IEEE international conference on local computer networks, pp. 455–462. IEEE (2004)
11. Estrin, A.C., Lagos Jenschke, T., Papadopoulos, G.Z., Ignacio Alvarez-Hamelin, J., Montavont, N.: Thorough Investigation of multipath Techniques in RPL based Wireless Networks. In: 2020 IEEE Symposium on Computers and Communications (ISCC), pp. 1–7 (2020). DOI 10.1109/ISCC50000.2020.9219646

12. Hou, J., Jadhav, R., Luo, Z.: Optimization of Parent-node Selection in RPL-based Networks. Internet-Draft draft-hou-roll-rpl-parent-selection-00, Internet Engineering Task Force (2017). URL https://datatracker.ietf.org/doc/html/draft-hou-roll-rpl-parent-selection-00. Work in Progress
13. Iova, O., Theoleyre, F., Noel, T.: Exploiting multiple parents in RPL to improve both the network lifetime and its stability. In: 2015 IEEE International Conference on Communications (ICC), pp. 610–616. IEEE (2015)
14. Kettouche, S., Maimour, M., Derdouri, L.: QoE-based performance evaluation of video transmission using RPL in the IoMT. In: 2019 7th Mediterranean Congress of Telecommunications (CMT), pp. 1–4 (2019). DOI 10.1109/CMT.2019.8931382
15. Khernane, N., Couchot, J.F., Mostefaoui, A.: Optimal power/rate trade-off for internet of multimedia things lifetime maximization under dynamic links capacity. Future Generation Computer Systems **93**, 737–750 (2019)
16. Kim, H.S., Kim, H., Paek, J., Bahk, S.: Load balancing under heavy traffic in RPL routing protocol for low power and lossy networks. IEEE Transactions on Mobile Computing **16**(4), 964–979 (2016)
17. Lagos Jenschke, T., Koutsiamanis, R.A., Papadopoulos, G.Z., Montavont, N.: ODeSe: On-demand selection for multi-path RPL networks. Ad Hoc Networks **114** (2021)
18. Liang, J., Tran, T.D.: A fast multiplierless approximations of the dct with the lifting scheme. IEEE Transactions on Signal Processing **49**(2), 3032–3044 (2001)
19. Liu, X., Guo, J., Bhatti, G., Orlik, P., Parsons, K.: Load balanced routing for low power and lossy networks. In: 2013 IEEE Wireless Communications and Networking Conference (WCNC), pp. 2238–2243 (2013). DOI 10.1109/WCNC.2013.6554908
20. Lodhi, M.A., Rehman, A., Khan, M.M., Asfand-e yar, M., Hussain, F.B.: Transient multipath routing protocol for low power and lossy networks. KSII Transactions on Internet & Information Systems **11**(4) (2017)
21. Maimour, M.: Interference-aware multipath routing for WSNs: Overview and performance evaluation. Applied Computing and Informatics (2018). URL http://www.sciencedirect.com/science/article/pii/S2210832717303009
22. Maimour, M.: SenseVid: A Traffic Trace based Tool for QoE Video Transmission Assessment Dedicated to Wireless Video Sensor Networks. Simulation Modelling Practice and Theory **87**, 120–137 (2018)
23. Maimour, M., Bidai, Z.: A multipath prefix routing for wireless sensor networks. Wireless Personal Communications **91**(1), 313–343 (2016)
24. Makkaoui, L., Lecuire, V., Moureaux, J.: Fast zonal dct-based image compression for wireless camera sensor networks. In: Image Processing Theory Tools and Applications (IPTA), 2010 2nd International Conference on, pp. 126–129 (2010). DOI 10.1109/IPTA.2010.5586798
25. Mammeri, A., Khoumsi, A., Ziou, D., Hadjou, B.: Modeling and adapting jpeg to the energy requirements of VSN. In: Computer Communications and Networks, 2008. ICCCN '08. Proceedings of 17th International Conference on, pp. 1–6 (2008). DOI 10.1109/ICCCN.2008.ECP.151
26. Moghadam, M.N., Taheri, H.: High throughput load balanced multipath routing in homogeneous wireless sensor networks. In: 2014 22nd Iranian Conference on Electrical Engineering (ICEE), pp. 1516–1521. IEEE (2014)
27. Mortazavi, F., Khansari, M.: An energy-aware RPL routing protocol for internet of multimedia things. In: Proceedings of the International Conference on Smart Cities and Internet of Things, SCIOT '18, pp. 11:1–11:6. ACM, New York, NY, USA (2018). DOI 10.1145/3269961.3269965. URL http://doi.acm.org/10.1145/3269961.3269965
28. Mostefaoui, A., Fawaz, Z., Noura, H.: A robust image-encryption approach against transmission errors in communicating things networks. Ad Hoc Networks **94**, 101,947 (2019)
29. Nauman, A., Qadri, Y.A., Amjad, M., Zikria, Y.B., Afzal, M.K., Kim, S.W.: Multimedia internet of things: A comprehensive survey. IEEE Access **8**, 8202–8250 (2020)
30. Romdhani, I., Qasem, M., Al-Dubai, A.Y., Ghaleb, B.: Cooja simulator manual. Tech. rep., Edinburgh Napier University (2016)
31. Sarif, B.A.B., Pourazad, M., Nasiopoulos, P., Leung, V.C.M.: A study on the power consumption of H.264/AVC-based video sensor network. International Journal of Distributed Sensor Networks **11**(10), 304,787 (2015). DOI 10.1155/2015/304787. URL https://doi.org/10.1155/2015/304787

32. Seeling, P., Reisslein, M., Kulapala, B.: Network performance evaluation using frame size and quality traces of single-layer and two-layer video: A tutorial. Communications Surveys Tutorials, IEEE **6**(3), 58–78 (2004)
33. Suseela, G., Asnath Victy Phamila, Y.: Energy efficient image coding techniques for low power sensor nodes: A review. Ain Shams Engineering Journal **9**(4), 2961 – 2972 (2018). DOI https://doi.org/10.1016/j.asej.2017.10.004. URL http://www.sciencedirect.com/science/article/pii/S2090447917301247
34. Tahir, Y., Yang, S., McCann, J.: BRPL: Backpressure RPL for high-throughput and mobile IoTs. IEEE Transactions on Mobile Computing **17**(1), 29–43 (2017)
35. Tang, W., Ma, X., Huang, J., Wei, J.: Toward improved RPL: A congestion avoidance multipath routing protocol with time factor for wireless sensor networks. Journal of Sensors (2016)
36. Taylor, C.N., Panigrahi, D., Dey, S.: Design of an adaptive architecture for energy efficient wireless image communication. In: Embedded processor design challenges, pp. 260–273. Springer (2002)
37. Telea, A.: An image inpainting technique based on the fast marching method. Journal of graphics tools **9**(1), 23–34 (2004)
38. Thubert, P.: Objective Function Zero for the Routing Protocol for LowPower and Lossy Networks (RPL). RFC 6552 (2012)
39. University, A.S.: YUV video sequences (2012). URL http://trace.eas.asu.edu/yuv/index.html
40. Vasseur, J., Kim, M., Pister, K., Dejean, N., Barthel, D.: Routing Metrics Used for Path Calculation in Low-Power and Lossy Networks. RFC 6551 (2012)
41. Wang, Z., Bovik, A., Sheikh, H., Simoncelli, E.: Image quality assessment: from error visibility to structural similarity. Image Processing, IEEE Transactions on **13**(4), 600–612 (2004). DOI 10.1109/TIP.2003.819861
42. Wang, Z., Zhang, L., Zheng, Z., Wang, J.: Energy balancing RPL protocol with multipath for wireless sensor networks. Peer-to-Peer Networking and Applications **11**(5), 1085–1100 (2018)
43. Zhu, L., Wang, R., Yang, H.: Multi-path data distribution mechanism based on rpl for energy consumption and time delay. Information **8**(4), 124 (2017)